Analytical Methods

Electrochemical detection of guaiacol in bamboo juice based on the enhancement effect of RGO nanosheets

Journal:	*Analytical Methods*
Manuscript ID:	AY-ART-01-2014-000195
Article Type:	Paper
Date Submitted by the Author:	22-Jan-2014
Complete List of Authors:	wu, yan; hubei institute for nationalities, huang, meng; hubei institute for nationalities, song, nannan; hubei institute for nationalities, hu, weibing; hubei institute for nationalities,

Electrochemical detection of guaiacol in bamboo juice based on the enhancement effect of RGO nanosheets

Yan Wu[a,b], Meng Huang[a,b], Nannan Song[b], Weibing Hu[a*]

[a] *Key Laboratory of Biological Resources Protection and Utilization of Hubei Province, Enshi 445000, China*

[b] *School of Chemical and Environmental Engineering, Hubei University for Nationalities, Enshi 445000, China*

Reduced graphene oxide (RGO) nanosheets with high quality were chemically synthesized by hydrothermal reduction of well-dispersed graphene oxide (GO) suspension. The electrochemical behavior of guaiacol was studied on different carbon materials surface. Compared with the bare glassy carbon, graphite, and GO, RGO nanosheets exhibited strong enhancement effect and the electrochemical oxidation response of guaiacol was remarkably improved. The influence of the pH value, amount of RGO, scan rate and accumulation time on the oxidation signal of guaiacol were investigated. Based on the enhancement effect of RGO, a simple, fast and sensitive electrochemical method was developed for the detection of guaiacol. The linear range was from 0.5 μM to 500 μM with a correlation coefficient of 0.998, and the limit of detection was as low as 0.2 μM (S/N = 3). Finally, it was used to determine guaiacol in bamboo juice sample, and the recovery was over the range

between 98.9% and 105.8%.

Keywords: RGO nanosheets; Guaiacol; Bamboo juice; Electrochemical detection.

Introduction

Graphene, a two dimensional monolayer of sp^2 carbon in a honeycomb-like network, has attracted a great deal of scientific interest in these years.[1-3] Due to its unique electric, thermal and mechanical characteristics, graphene has been extensively applied in many technological fields such as transparent conducting films,[4] sensors,[5] supercapacitors,[6] and batteries.[7] Up to now, various approaches have been developed for the synthesis of graphene, including mechanical exfoliation,[8] epitaxial growth,[9] chemical vapor deposition,[10] unzipping carbon nanotubes,[11] liquid phase exfoliation of graphite,[12] chemical reduction of GO,[13] etc. According to data, graphene prepared through chemical reduction of GO possesses many structural defects, which are advantageous for the electrochemical sensing, for example, the response signals and detection sensitivity of glucose,[14] H_2O_2,[15] and NO_2[16] were enhanced remarkably on the surface of RGO nanosheets.

Guaiacol is a kind of natural organic matter which is the major ingredient of creosote. Because of the special pharmacological effects such as strong anti-microbial action, anti-inflammation action and anti-nociceptive action, guaiacol was widely used in the field of medicine.[17,18] Therefore, the detection of guaiacol is quite important and interesting. Liquid chromatography-mass spectrometry[19] and gas

chromatography-mass spectrometry[20] are the most common approaches for the detection of guaiacol. Although electrochemical method possesses the advantages such as high sensitivity, short analysis time, low cost and handling convenience, the electrochemical detection of guaiacol is limited. As shown in Fig. 1, the structural formula of guaiacol contains phenolic hydroxyl group and should be electrochemical active, even so, electrochemical determination of guaiacol using RGO nanosheets has not been reported.

The main objective of this work is to study the electrochemical response of guaiacol on the surface of RGO and then develop a simple, rapid and sensitive electrochemical method for the detection of guaiacol utilizing the unique property of RGO nanosheets. RGO nanosheets were synthesized by using $Na_2S_2O_3$ as the reducing reagent from graphene oxide through hydrothermal method. The obtained RGO was well-dispersed in water, resulting in a stable and homogeneous suspension. Compared with the bare GCE, GO and the RGO modified electrodes, RGO greatly improves the oxidation signal of guaiacol, indicating that RGO exhibits remarkable surface enhancement effect toward the oxidation of guaiacol. Based on this, a sensitive and convenient electrochemical method was proposed for the determination of guaiacol, which was successfully demonstrated with traditional Chinese medicines of bamboo juice.

Experimental section

Reagents

All chemicals were of analytical grade and used as received. Guaiacol was obtained from Guangfu fine chemical insititute (Tianjin, China). $KMnO_4$, sulphuric acid (98%), graphite powder (99.99% purity, ~100 mesh), and $Na_2S_2O_3 \cdot 5H_2O$ were purchased from Zhongtian chemical reagent company (Wuhan, China). Absolute ethyl alcohol and absolute ether were obtained from Fuchen chemical reagent company (Tianjin, China).

Instruments

The electrochemical measurements were performed using 660D electrochemical analyzer (CH Instruments, USA) with a conventional three-electrode system. The working electrode was RGO modified glassy carbon electrode, the reference electrode an Ag/AgCl with saturated KCl, and the counter electrode was a Pt wire. Scanning electron microscopy (SEM) was performed with a JEOL microscope (JSM-6510LV, Japan). Transmission electron microscopy (TEM) images were measured using a Tecnai G220 microscope (FEI Company, Netherlands). Raman spectra were carried out on a LabRAM HR800 confocal Raman microscopy using 532 nm laser (Horiba JobinYvon, France). Fourier Transform Infrared spectroscopy (FTIR) were obtained with a Avatar 360 spectrometer (Nicolet, America) with a KBr plate. X-ray diffraction (XRD) patterns were measured using a diffractometer (Shimadzu XRD-7000, Japan) The ultraviolet spectrum measurement was carried out with TU-1901 (Persee corporation of beijing, China).

Synthesis of GO and RGO

Graphene oxide, was synthesized by Hummer's method.[21] RGO used in this work was prepared by the chemical reduction of GO with $Na_2S_2O_3 \cdot 5H_2O$. In brief, 50 mg GO was first ultrasonically dispersed in 80 mL H_2O for 1.5 h to get graphene oxide suspension, then 0.5 g $Na_2S_2O_3 \cdot 5H_2O$ was added into the GO suspension. The mixture was then sealed into a Teflon-lined stainless steel autoclave and maintained at 180 ºC for 24 h. After it was cooled down to the room temperature, the resulting product was separated by centrifugation, washed with deionized water and ethanol for several times, and dried at 60 ºC under vacuum overnight.

Fabrication of RGO modified GCE

RGO nanosheets (10.0 mg) were added into doubly distilled water (10.0 mL), and then sonicated in a KQ3200DE ultrasonicator for 1 h, giving a stable and black graphene suspension. Before modification with RGO, the GCE with a diameter of 3 mm was polished with 0.05 mm alumina slurry, and then sonicated in doubly distilled water for 2 min. After drying, the GCE surface was coated with 10 μL RGO suspension, and the water was evaporated under an infrared lamp in air. The RGO nanosheets modied GCE was prepared. For the comparasion, 1 mg/mL graphite and GO suspension was also prepared to modify the glassy carbon electrode, respectively.

Sample preparation

The bamboo juice (pharmaceutical co., LTD of tongyuan Sichuan, China) used in this study was purchased from a local pharmacy. The extraction process of guaiacol was

performed as described like this. Briefly, the pH of 60 mL bamboo juice was adjusted close to 1~2. 20 mL ether was added into the above solution and the extraction process parallelly undergoes 3 times, then the ether extraction solution was mixed together. The mixture of the ether extraction solution was washed with 50 mL 5% $NaHCO_3$ for 3 times, the layer of $NaHCO_3$ solution was abandoned and the final ether extraction solution was gathered. The ether in the final extraction solution was evaporated at room temperature. Finally, the remaining residue was dissolved in 25 ml ethanol for measurement.

Analytical procedure

Unless otherwise stated, 0.1 M, pH 6.5 phosphate buffer (PBS) was used as the supporting electrolyte for the detection of guaiacol. After 30 s accumulation, the differential pulse voltammetry (DPV) curves were recorded from 0.1 to 1.0 V, and the oxidation peak current at 0.60 V was measured for guaiacol. The pulse amplitude is 50 mV, pulse width is 40 ms, and the scan rate is 40 mV s^{-1}.

Results and discussion

AFM Characterization of GO and RGO

RGO together with the original GO were first examined by AFM. As shown in Fig. 2, the mean thickness of GO is about 1.24 nm (a) and RGO is 1.41 nm (b), the small distinction in thickness between GO an RGO, suggesting the original GO and the obtained RGO possess the same layers. The theoretical thickness for a perfectly flat,

single layer sp^2-carbon atom netwok is about 0.3 nm, so it can be concluded that the number of layers of the synthesized RGO is about 4.

The morphologies of different carbon materials were further characterized by SEM and TEM. As shown in Fig. 4A, the unmodified GCE surface was smooth and virtually featureless. On the other hand, the pristine graphite was made of large bulk particles in micron meter as displayed in Fig. 4B. After modification with GO nanosheets as illustrated in Fig. 4C, wrinkled sheets were observed. In addition, the RGO film demonstrated a curly and corrugated appearance consisting of a wrinkling paper-like structure, which is significantly different from the flat and characterless GCE surface. To preferably check the microstructure, TEM test was also performed for GO and RGO. Fig. 3E and 4F are TEM images of GO and RGO. It was clear that both of GO and RGO exhibited wrinkled flake-like shapes. The wrinkled nature of graphene is highly beneficial in maintaining a high surface area, which is advantageous to improve the accumulation efficience of the target analyte in electrochemical sensing.

Enhancement effect of RGO nanosheets

The electrochemical behavior of guaiacol was studied on the unmodified, graphite-modified, GO-modified and RGO-modified GCEs using cyclic voltammetry (CV). Fig. 4 shows the electrochemical response of 50 μM guaiacol on different electrode surface in 0.1 M (pH 6.5) phosphate buffer solution. Successive cyclic sweep was conducted from 0 to 1.0 V, the oxidation peak current was recorded as the

analytical signal. The electrochemical signals on the un-modified GCE (black line) and graphite modified GCE (red line) were negligible, indicating the oxidation activity of guaiacol on unmodified and graphite-modified GCEs was very low. When using GO-modified GCE (blue line), a small oxidation peak appeared at about 0.60 V, suggesting that GO is more active to the electrochemical detection compared with the unmodified and graphite-modified GCEs. What interesting is that when RGO-modified GCE was used, a well-defined oxidation peak at about 0.63 V was observed (green line), and the peak current increased greatly relative to GO-modified GCE. The notable peak current enhancement indicates that RGO nanosheets can greatly accelerate the electron transfer rate. The strong enhancement effect toward the oxidation of guaiacol may attribute to the superior electroconductivity, huge specific area and strong accumulation efficience of RGO.

To explain the different activities of GO and RGO toward the oxidation of guaiacol, the surface functional group of pristine graphite, GO and RGO was investigated by FTIR. Fig. 5 shows the FTIR spectra of graphite (curve a), RGO (curve b) and GO (curve c). After chemical oxidation of pristine graphite, numerous oxygen-containing functional group was introduced on the surface of GO (curve c), such as O-H (3428 cm^{-1}), C=O (1724 cm^{-1}), C=C (1635 cm^{-1}) and alkoxy C-O (1045 cm^{-1}). Compared with GO, the peak at 1724 cm^{-1}(C=O), 1250 cm^{-1} (epoxy C-O) and 1400 cm^{-1} (carboxy C-O) significantly decreased on RGO surface, indicating the effective reduction of the GO. Of course, part of oxygen-containing functional group still existed on the surface of RGO though most of the functional groups in GO were

removed, which was similar to the other report.[22]

The element contents of graphite, GO and RGO were analyzed using XPS. Fig. 6 displays the XPS spectra of graphite, GO and RGO. For graphite, the content of oxygen was as low as 2.60% and the content of carbon was as high as 97.40%. On the other hand, the content of oxygen remarkably increased to 32.57% for GO. However, the oxygen content decreased greatly to 15.44% for RGO compared with GO, suggesting considerable deoxygenation by the hydrothermal reduction process. Moreover, no extra elements than oxygen and carbon were detected, suggesting the purity of graphite, GO and RGO was very high. From the FTIR and XPS spectra, we know that RGO was successfully reduced from GO through the hydrothermal process.

To obtain further information on the structure of RGO, Raman spectra was carried out. Fig. 7 shows the Raman spectra of pristine graphite (a), GO (b) and RGO (c). As shown in Fig. 7a, two obvious peaks at 1580 cm^{-1} and 2700 cm^{-1} were observed for the pristine graphite, which was assigned to the G-band and 2D-band of the natural graphite.[23] Additionally, a small peak at 1350 cm^{-1} was also examined which was attributed to the disorder-related D-band. According to data, the D band is due to the existence of defects in basal plane and edge of carbon material, and its intensity is linked with the amount of disorder.[24,25] The tiny D-band intensity (I_D) suggests that few defects existed in pristine graphite. However, the D-band became well-defined and the intensity increased obviously in the spectra of GO and RGO. The greatly-increased D-band indicats great deal of defects existed in basal plane and edge of graphene than in graphite. On the other hand, the relative intensity ratio of the D

and G (I_D/I_G ratio) is proportional to the number of defect sites in graphite carbon.[24] Compared with GO, an increased I_D/I_G intensity ratio can be observed for RGO, indicating there are more defective sites existing on the surface of RGO, which may be the reason of higher activity toward the oxidation of guaiacol relative to GO and the pristine graphite.

Fig. 8 shows the X-ray diffraction (XRD) patterns of graphite, GO and RGO nanosheets. A very sharp peak was observed at $2\theta = 26.5°$ for graphite (curve a), which attributes to the diffraction of (002) plane, and the interlayer distance obtained from the (002) plane was 3.48Å. A typical oxidation leads to the appearance of diffraction peak of the GO at $2\theta = 10.8°$ without the peak of d_{002} visible in graphite due to the introduction of oxygen-containing groups to the graphite surface,[26] and the corresponding interlayer distance was calculated to be 8.37 Å. In the case of RGO, only a broad peak at $2\theta = 23.4°$ can be observed, and the interlayer distance was 3.63 Å, indicating a sufficient reduction process of the original graphene oxide.[26]

Effect of pH and scan rate on the oxidation of guaiacol at RGO/GCE

In order to optimize the response of guaiacol at RGO/GCE, some different supporting electrolytes such as phosphate buffer solution, Tris buffer solution, acetate buffer solution, B-R buffer solution, HCl and $HClO_4$ solution was discussed by cyclic voltammetry. The results indicate that the peak current of guaiacol in 0.1 M phosphate buffer solution is larger than in the others (data not shown), so phosphate buffer solution was chosen as the supporting electrolyte. The effect of phosphate buffer

solution with different pH values ranging from 5.7 to 8.0 on the oxidation response of 10 μM guaiacol was investigated. It was found that E_{pa} was depended on the solution pH. A good linear relationship was obtained between the E_{pa} and pH. The liner regression equation is E_{pa}/V = 1.037-0.0624pH, and the correlation coefficient is 0.995. According to the relationship between the peak potential and pH, the slope of -62.4 mV/pH indicated that the electron transfer was accompanied by an equal number of protons in the electrode reaction process.[27] In addition, the maximum current response of guaiacol was obtained at pH 6.5 phosphate buffer solution. Therefore, pH 6.5 phosphate buffer solution was chosen for the subsequent analytical experiments.

The influence of scan rate (v) on the oxidation of guaiacol at the RGO/GCE was investigated by linear sweep voltammetry (LSV). In pH 6.5 phosphate buffer solution, the anode peak current of guaiacol increased continuously with the increase of scan rate (v) over the range from 0.05 to 0.25 V s^{-1}. A good linear relationship between the peak current and square root of the scan rate ($v^{1/2}$) was obtained. The linear regression equation is i_{pa}(μA) = -0.2739+30.3315$v^{1/2}$ (v in V s^{-1}), and the correlation coefficient is 0.995, indicating the oxidation of guaiacol was controlled by diffusion. Moreover, according to Fig. 4, only an oxidation peak was observed, indicating that the oxidation of guaiacol was a totally irreversible electrode process.

Additionally, the E_{pa} of guaiacol shifted positively with increasing the scan rate. The dependence of E_{pa} with ln v can be expressed as E_{pa} (V) = 0.74926+0.06548ln v (V s^{-1}), and the correlation coefficient is 0.995. As for an irreversible electrode

process, according to Laviron,[28] E_{pa} is defined by the following equation: $E_p = E^0 - (RT/\alpha nF)\ln(\alpha nF/RTk_s) - (RT/\alpha nF)\ln v$, where α is the electrontransfer coefficient, n is the electron-transfer number, k_s is the rate constant of the reaction, v is the scan rate and E^0 is the formal redox potential. So the value of n can be easily calculated from the slope of E_p versus ln v. Here, taking R = 8.314, T = 298 and F = 96500, generally, α is assumed to be 0.5 in a totally irreversible electrode process, so it can be calculated that one electron and one proton was involved in the oxidation of guaiacol.

Detection of guaiacol using RGO/GCE

Fig. 9 shows the influence of the amount of RGO suspension on the oxidation peak current of 5 μM guaiacol using differential pulse voltammetry (DPV). After 30 s accumulation under open circuit, the oxidation peak current was recorded as the analytical singal. The oxidation peak current of guaiacol increased remarkably with the volume of RGO suspension over the range from 0 to 10 μL. During this period, the accumulation efficiency of RGO/GCE obviously enhanced. However, the oxidation current gradually decreased when further improving the amount of RGO, which may be due to the block effect of RGO for the decreased electric conductivity. In order to shorten the time of solvent evaporation and to achieve high sensitivity, 10 μL RGO suspension was used to modify the GCE surface.

Fig. 10 displays the effect of accumulation time on the oxidation peak current of 50 μM guaiacol. By extending the accumulation time from 0 to 30 s, the oxidation peak current increased greatly, revealing that accumulation is efficient to improve the

detection sensitivity. It is a surprise that longer accumulation time than 30 s does not enhance the oxidation peak current, suggesting that the amount of guaiacol on the surface of RGO tends to a limiting value. Considering sensitivity and analysis time, 30 s accumulation was employed.

The RGO modified GCE was used for single determination in this work. The reproducibility for multiple modified GCEs was estimated by measuring the peak current of 5 μM guaiacol. For 5 RGO modified GCEs, the value of the relative standard deviation (RSD) was 3.2%, suggesting excellent fabrication reproducibility and detection precision.

The potential interferences for the determination of guaiacol were examined. Under the optimized conditions, the oxidation peak current of 5 μM guaiacol was individually measured in the presence of different concentrations of interferents, and then the peak current change was checked. No influence on the detection of guaiacol was observed after the addition of 500-fold amounts of Cu^{2+}, Fe^{3+}, Mg^{2+}, Zn^{2+}, Pb^{2+}, 100-fold amounts of the pyrogallol, resorcinol, phenole (peak current change was below 5%).

The linear range and limit of detection were tested using DPV under the optimized conditions. As displayed in Fig. 11, the oxidation peak current of guaiacol (i_p, μA) was linear with its concentration (C, μM) over the range from 0.5 to 500 μM, obeying the following linear equation: i_p = 0.06898 C+4.725. The correlation coefficient was 0.998, suggesting good linearity. After 30 s accumulation under open circuit, the limit of detection was evaluated to be 0.2 μM based on three signal to

noise ratio.

Analytical application

To demonstrate its applicability of the proposed method for real sample analysis, bamboo juice sample was used for the quantitative analysis. Each sample solution undergoes five parallel detections, and the RSD was below 5%. The concentration of guaiacol was obtained by the standard addition method, and the results are listed in Table 1. In order to testify the accuracy of this method, the content of guaiacol was also analyzed using ultraviolet spectrum. The obtained results are in good agreement, revealing that this method is satisfactory. In addition, a known amount of guaiacol standard was spiked in the sample, and then analyzed according to the same procedure. The value of recovery was in the range from 98.9% to 105.8%, also indicating that determination of guaiacol using RGO modified GCE is accurate and feasible.

Conclusion

RGO nanosheets with high quality were chemically synthesized by hydrothermal reduction of well-dispersed GO suspension. Compared with glassy carbon, graphite and GO, RGO remarkably increased the peak current toward the oxidation of guaiacol. Based on the great enhancement effect of RGO nanosheets, a rapid, sensitive and convenient electrochemical method was developed for the detection of guaiacol. This method was successfully used in bamboo juice sample, and revealed promising application.

Acknowledgements

This work was supported by Open Foundation of Key Laboratory of Biologic Resources Protection and Utilization of Hubei Province, Forestry Key Disciplines (No.PKLHB1303), the National Natural Science Foundation of China (No. 20871044).

References

1 J.L. Achtyl, I.V. Vlassiouk, P.F. Fulvio, S.M. Mahurin, S. Dai, F.M. Geiger, *J. Am. Chem. Soc.*, 2013, **135**, 979-981.

2 B. Zhang, L.X. Fan, H.W. Zhong, Y.W. Liu, S.L. Chen, *J. Am. Chem. Soc.*, 2013, **135**, 10073-10080.

3 A.K. Geim, K.S. Novoselov, *Nat. Mater.*, 2007, **7**, 6183-6191.

4 X. Wang, L.J. Zhi, K. Müllen, *Nano Lett.*, 2008, **8**, 323-327.

5 Z.G. Cheng, Q. Li, Z.J. Li, Q.Y. Zhou, Y. Fang, *Nano. Lett.*, 2010, **10**, 1864-1868.

6 H.L. Wang, Q.L. Hao, X.J. Yang, L.D. Lu, X. Wan, *Electrochem. Commun.*, 2009, **11**, 1158-1161.

7 C.Y. Wang, D. Li, C.O. Too, *Chem. Mater.*, 2009, **21**, 2604-2606.

8 S.P. Pang, J.M. Englert, H.N. Tsao, Y. Hernandez, A. Hirsch, X.L. Feng, K. Müllen, *Adv. Mater.*, 2010, **22**, 5374-5377.

9 H. Huang, W. Chen, S. Chen, A.T.S. Wee, *ACS Nano*, 2008, **2**, 2513-2518.

10 A. Reina, X.T. Jia, J. Ho, D. Nezich, H. Son, V. Bulovic, M.S. Dresselhaus, J.

Kong, *Nano. Lett.*, 2009, **9**, 30-35.

11 D.B. Shinde, J. Debgupta, A. Kushwaha, M. Aslam, V.K. Pillai, *J. Am. Chem. Soc.*, 2011, **133**, 4168-4171.

12 G.X. Wang, B. Wang, J. Park, Y. Wang, B. Sun, J. Yao, *Carbon*, 2009, **47**, 3242-3246.

13 M. Zhou, Y.M. Zhai, S.J. Dong, *Anal. Chem.*, 2009, **81**, 5603-5613.

14 X. Chen, H. Ye, W. Wang, B. Qiu, Z. Lin, G. Chen, *Electroanalysis*, 2010, **22**, 2347-2352.

15 Q. Lu, X. Dong, L.J. Li, X. Hu, *Talanta.*, 2010, **82**, 1344-1348.

16 J.D. Fowler, M.J. Allen, V.C. Tung, Y. Yang, R.B. Kaner, B.H. Weiller, *ACS Nano.*, 2009, **3**, 301-306.

17 T. Ohkubo, M. Shibata, *J. Dent. Res.*, 1997, **76**, 848-851.

18 H.F. Liu, B. Lepoittevin, C. Roddier, V. Guerineau, L. Bech, J.M. Herry, M.N. Bellon-Fontaine, P. Roger, *Polymer*, 2011, **52**, 1908-1916.

19 M. Takahashi, S. Sakamaki, A. Fujita, *Biosci. Biotechnol. Biochem.*, 2013, **77**, 595-600.

20 P.R. Pérez-Cacho, M.D. Danyluk, R. Rouseff, *Food Chem.*, 2011, **129**, 45-50.

21 W.S. Hummers, R.E. Offeman, *J. Am. Chem. Soc.*, 1958, **80**, 1339-1340.

22 C. Wu, D. Sun, Q. Li, K.B. Wu, *Sens. Actuator B-Chem.*, 2012, **168**, 178-184.

23 A.C. Ferrari, J. Robertson, *Phil. Trans. Roy. Soc. A.*, 2004, **362**, 2269-2270.

24 F. Tuinstra, J.L. Koenig, *J. Chem. Phys.*, 1970, **53**, 1126-1130.

25 A.C. Ferrari, J. Robertson, *Physical Review B*, 2000, **61**, 14095-14107.

26 C. Hontoria-Lucas, A.J. López-Peinado, J.D.D. López-González, M.L. Rojas-Cervantes, R.M. Martín-Aranda, *Carbon*, 1995, **33**, 1585-1592.

27 F.Y. Zhang, Z.H. Wang, Y.Z. Zhang, Z.X. Zheng, C.M. Wang, Y.L. Du, W.C. Ye, *Talanta*, 2012, 93, 320-325.

28 E. Laviron, *J. Electroanal. Chem.*, 1974, **52**, 355-393.

Captions for figures and table

Fig. 1 Structural formula of guaiacol.

Fig. 2 AFM images of GO (a) and RGO nanosheets (b).

Fig. 3 SEM images of GCE (A), graphite (B), GO (C) and RGO (D); TEM images of GO (E) and RGO (F).

Fig. 4 CV curves of 50 μM guaiacol on the unmodified GCE (black line), graphite-modified GCE (red line), GO-modified (blue line) and RGO-modified (green line) GCEs. Scan rate: 100 mV s^{-1}.

Fig. 5 FTIR spectra of graphite (a), RGO (b) and GO (c).

Fig. 6 XPS spectra of graphite, GO and RGO.

Fig. 7 Raman spectra of Graphite, GO and RGO.

Fig. 8 The picture of XRD: graphite (a), GO(b) and RGO (c).

Fig. 9 Influence of amount of RGO suspension on the oxidation peak current of 5 μM

guaiacol.

Fig. 10 Influence of accumulation time on the oxidation peak current of 50μM guaiacol.

Fig. 11 DPV curves of guaiacol with different concentrations on RGO modified GCE. (a) 0 μM, (b) 2 μM, (c) 5 μM, (d) 10 μM, (e) 50 μM, (f) 105 μM and (g) 200 μM.

Table 1 Determination of guaiacol in bamboo juice.

Fig. 1

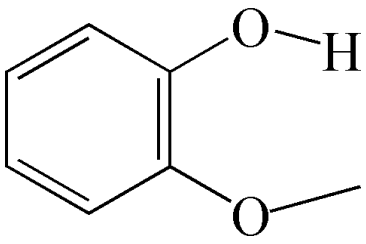

Fig. 2

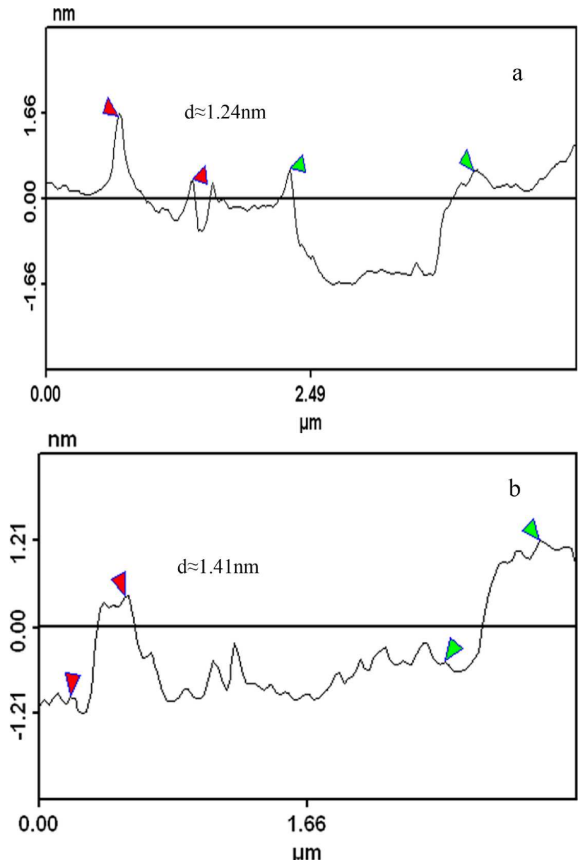
nm
a
d≈1.24nm
1.66
0.00
-1.66
0.00
2.49
μm
nm
b
d≈1.41nm
1.21
0.00
-1.21
0.00
1.66
μm

Fig. 3

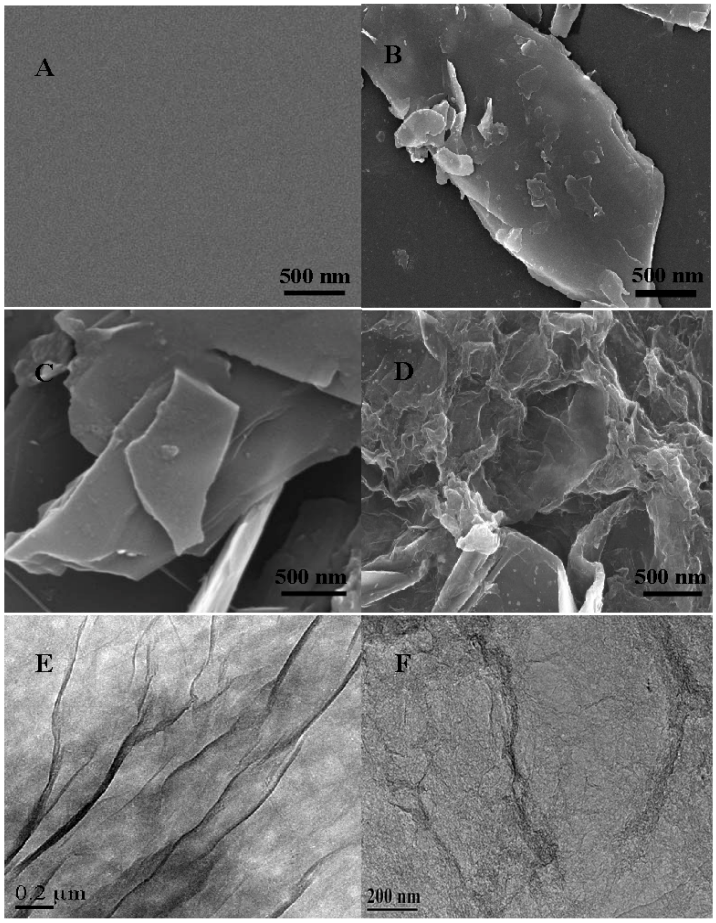

Fig. 4

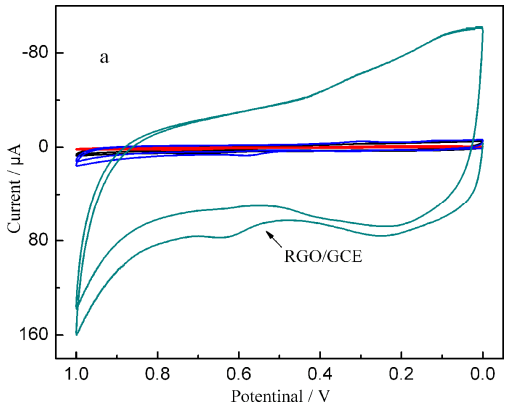

Fig. 5

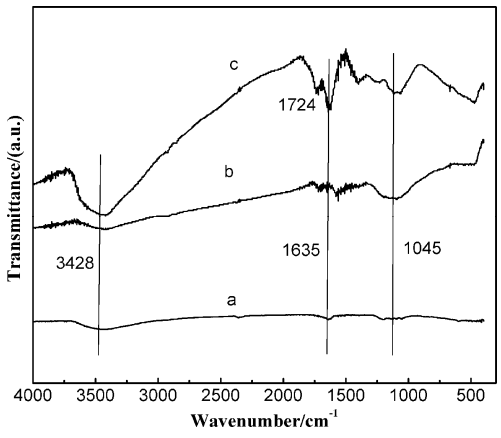
c
1724
b
3428
1635
1045
a
Transmittance/(a.u.)
4000 3500 3000 2500 2000 1500 1000 500
Wavenumber/cm-1

Fig. 6

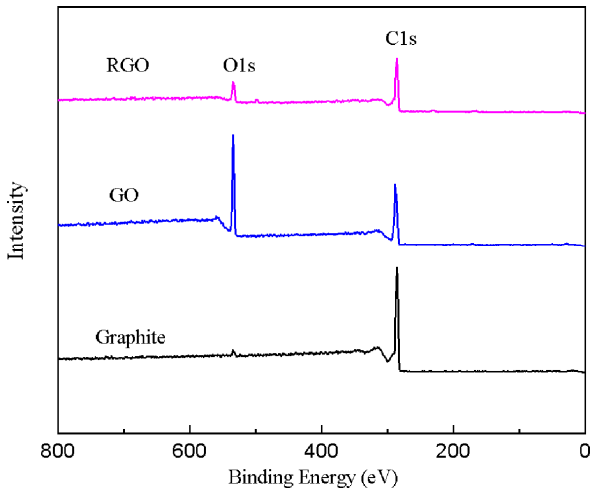
C1s
RGO
O1s
GO
Graphite
Intensity
800
600
400
200
0
Binding Energy (eV)

Fig. 7

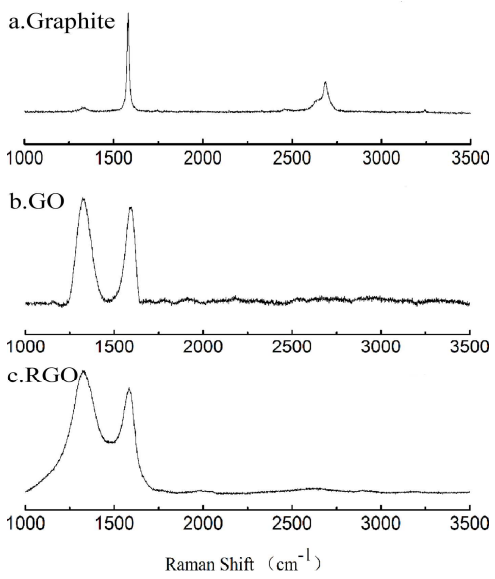
a.Graphite
1000
1500
2000
2500
3000
3500
b.GO
1000
1500
2000
2500
3000
3500
c.RGO
1000
1500
2000
2500
3000
3500
Raman Shift （cm-1）

Fig. 8

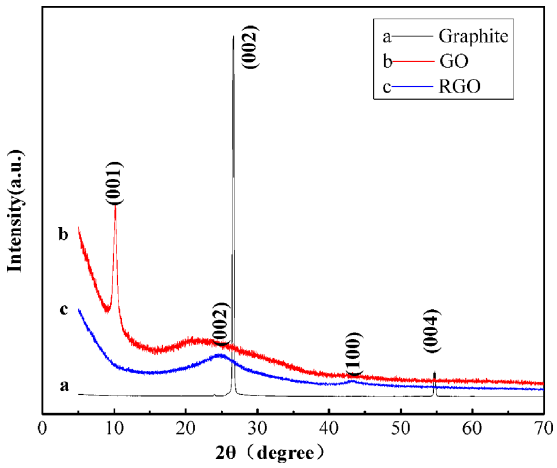
a Graphite
b GO
c RGO
(002)
(001)
(002)
(100)
(004)
b
c
a
Intensity(a.u.)
0
10
20
30
40
50
60
70
2θ（degree）

Fig. 9

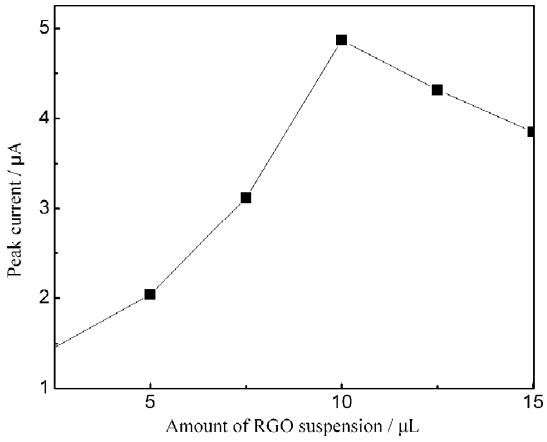

Fig. 10

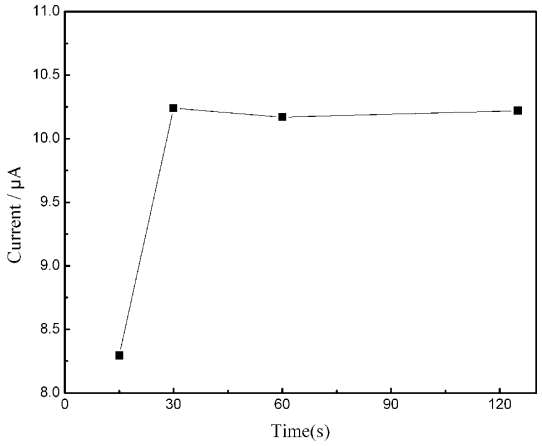

Fig. 11

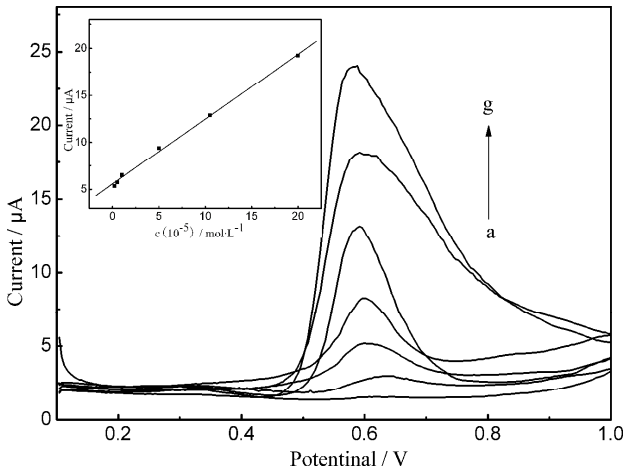

Table 1 Determination of guaiacol in bamboo juice.

Sample	UV (M)	This method (M)	Recovery (%)	RSD (%,n=5)
A	5.07×10^{-6}	5.29×10^{-6}	105.8	1.2
B	6.72×10^{-5}	6.96×10^{-5}	99.4	4.5
C	2.59×10^{-4}	2.67×10^{-4}	98.9	3.6

Reduced graphene oxide (RGO) nanosheets with high quality were chemically synthesized by hydrothermal reduction of well-dispersed graphene oxide (GO) suspension. The electrochemical behavior of guaiacol was studied on different carbon materials surface. Compared with the bare glassy carbon, graphite, and GO, RGO nanosheets exhibited strong enhancement effect and the electrochemical oxidation response of guaiacol was remarkably improved.